Amino acid starvation inhibits autophagy in lipid droplet-deficient cells through mitochondrial dysfunction

Pierre Voisin, Marianne Bernard, Thierry Bergès, Matthieu Régnacq

Amino acid starvation inhibits autophagy in lipid droplet-deficient cells through mitochondrial dysfunction.

Pierre Voisin, Marianne Bernard, Thierry Bergès and Matthieu Régnacq *

From Laboratoire Signalisation & Transports Ioniques Membranaires (STIM) EA7349 Université de Poitiers, Bâtiment B31, 3 rue Jacques Fort, TSA51106, 86073 Poitiers Cedex 9, France

* To whom correspondence should be addressed; matthieu.regnacq@univ-poitiers.fr
Tel. (33)5 49 45 38 64

Running title

Autophagy requires functional lipid droplets and mitochondria

Abbreviations

ATG, autophagy-related gene; eIF2, eukaryotic initiation factor; ER, endoplasmic reticulum; GAAC, general amino acid control; GCN, general control nonderepressible; GSH, glutathione reduced form; GSSG, glutathione oxidised form; PtdCho, phosphatidylcholine; PtdIns, phosphatidylinositol; ROS, reactive oxygen species; STE, sterylester; TAG, triacylglycerol; TORC, target of Rapamycin complex.

Keywords

Autophagy; lipid droplets; *Saccharomyces cerevisiae*; mitochondria; catabolite repression.

Abstract

Lipid droplets are ubiquitous organelles in eukaryotes that act as storage sites for neutral lipids. Under normal growth conditions they are not required in the yeast *Saccharomyces cerevisiae*. However, recent works have shown that lipid droplets are required for autophagy to proceed in response to nitrogen starvation and that they play an essential role in maintaining ER homeostasis. Autophagy is a major catabolic pathway that helps degradation and recycling of potentially harmful proteins and organelles. It can be pharmacologically induced by rapamycin even in the absence of lipid droplets. Here, we show that amino acid starvation is responsible for autophagy failure in lipid droplet-deficient yeast. It not only fails to induce autophagy but also inhibits rapamycin-induced autophagy. The general amino acid control pathway is not involved in this paradoxical effect of amino acid shortage. We correlate the autophagy failure with mitochondria aggregation and we show that amino acid starvation-induced autophagy is restored in lipid droplet-deficient yeast by increasing mitochondrial biomass physiologically (respiration) or genetically (*REG1* deletion). Our results establish a new functional link between lipid droplets, ER and mitochondria during nitrogen starvation-induced autophagy.

Introduction

Macroautophagy (hereafter referred to as autophagy) is a major cellular response to maintain homeostasis [1]. It is induced in response to nutritional stress and results in bulk turnover of cytoplasmic content which ultimately allows the cell to adapt to a changing environment [2]. Research in the yeast *Saccharomyces cerevisiae* has significantly contributed to identifying genes responsible for autophagy, the so-called *ATG* genes (autophagy-related). Autophagy begins with the formation of a cup-shaped membrane structure called the isolation membrane, or phagophore, which expands and encapsulates the cytoplasmic macromolecules or organelles that are to be degraded [3]. The phagophore eventually closes to form a double membrane structure called the autophagosome [3]. Its content is then delivered to the lysosome - or vacuole in yeast - for degradation. Several cellular structures have been proposed as contributing to autophagosome biogenesis by providing lipids required for membrane expansion. These include the ER (endoplasmic reticulum), the Golgi apparatus, ER exit sites, endosomes, mitochondria and plasma membrane [4]. Recently, lipid droplets have also been shown to participate in autophagosome biogenesis in HeLa cells [5]. Although a direct contribution of lipid droplets to autophagosome membrane expansion in yeast is still controversial, several studies have pointed to a functional link between lipid droplets and autophagy [6-9].

Lipid droplets are cellular organelles filled with neutral lipids (*i.e.* TAG (triacylglycerols) and STE (steryl esters)) and delimited by a monolayer of phospholipids with associated proteins [10]. A yeast mutant has been generated that is unable to synthesize TAG and STE, resulting in the complete lack of lipid droplets [11] (Supplemental Figure 1). This mutant is viable, although it is highly sensitive to excess unsaturated fatty acids which cause mitochondrial dysfunction and necrotic cell death [12-14]. In addition, this mutant is unable to achieve autophagy in response to nitrogen starvation and the autophagy blockade in starved

cells is accompanied by the formation of membrane tangles initially observed in electron microscopy [7, 8]. The autophagy failure in lipid droplet-deficient cells was originally interpreted as a possible requirement for fatty acids generated by TAG or STE hydrolysis in autophagosome membrane biogenesis [6, 8]. This view was, however, challenged by two observations. Firstly, rapamycin, a potent inhibitor of TORC1 (Target of Rapamycin complex 1), was very efficient at inducing autophagy in the lipid droplet-deficient mutant, a result indicating that autophagy is not strictly dependent on lipid droplets [7, 9]. Secondly, nitrogen starvation - but not rapamycin - caused an increase in fatty acid biosynthesis and an alteration of phospholipid composition that proved detrimental to autophagy [7, 9]. In fact, the partial inhibition of fatty acid synthesis by cerulenin, or experimental elevation of the PtdCho (phosphatidylcholine)/PtdIns (phosphatidylinositol) ratio, restored autophagy in response to nitrogen starvation and also eliminated the membrane tangles [7, 9]. Thus, the inability of the lipid droplet-deficient mutant to buffer free fatty acid into lipid droplets or its inadequate phospholipid composition appeared more likely to be responsible for the autophagy defect. Restoration of autophagy by cerulenin or by PtdCho/PtdIns clamp was, however, only partial when compared to the intense autophagy triggered by rapamycin, suggesting that the mechanism of impairment had not been fully addressed. To gain access to this mechanism, a better definition of the origin of the problem appeared to be required. One question that arose was whether the absence of autophagy upon nitrogen starvation was a simple failure to activate the process or if it reflected an inhibitory mechanism capable of blocking the autophagic response to other kinds of stress (*i.e.* rapamycin). Another aspect of the situation that had not been examined is the fact that nitrogen starvation is a composite stress in a medium lacking both ammonium ion and amino acids. Previous studies in lipid droplet-proficient yeast have shown that ammonium ion deficiency and amino acid deficiency induce autophagy through different mechanisms and have different requirements for the General

Amino Acid Control (GAAC) pathway [15]. To obtain a better definition of the situation encountered in lipid droplet-deficient yeast, we sought to examine separately the effects of ammonium ion or amino acid deficiencies on autophagy.

Here, we show that ammonium ion deficiency induces autophagy in lipid droplet-deficient yeast (RS4Δ strain). In contrast, amino acid deficiency not only fails to activate autophagy but also inhibits the responses to ammonium deficiency and to rapamycin. Amino acid starvation also alters mitochondrial morphology. We report that this phenotype is dependent upon the carbon source present in the medium since it is observed in glucose-grown cells, but not in respiratory medium. Finally, we show that this phenotype can also be suppressed by deletion of the *REG1* gene which is necessary for carbon catabolite repression in glucose-grown cells.

Materials and methods

Strains, oligonucleotides, plasmids and growth conditions

All yeast strains described in this study are derived from BY (Euroscarf). BY4742 was used as the wild type strain (Y10000). RS4Δ (BY4742 derivative; *MATα are1 are2 lro1 dga1 ura3 trp1 leu2 lys2 his3 met15*) was kindly provided by Dr Schneiter. Deletions of *REG1* and *GCN2* were performed by PCR-based targeted homologous recombination, replacing the entire ORF with the *URA3* cassette [16]. PCR-mediated GFP tagging of *SEC63* was performed as described with pYM28 [17]. Plasmid pSu9-GFP expresses GFP fused to the presequence of subunit 9 of the F_0-ATPases of *Neurospora crassa* from the *ADH1* promoter. This plasmid is based on pRS315 and was kindly provided by Dr Sesaki [18]. For GFP-Atg8 processing, the plasmid pRS416 expressing GFP-Atg8 that was used [19] was kindly provided

by Dr Camougrand. Plasmid pPHY2427, expressing 3xHA-Atg13 under the control of the *CUP1* promoter in pRS426, was kindly provided by Pr Hermann [20].

Yeast strains were cultured in minimal YNB medium (yeast nitrogen base with ammonium sulfate and 2% glucose) supplemented with the appropriate Dropout mix (Formedium), or complete YPD medium (1% yeast extract, 1% peptone, 2% dextrose). Growth in respiratory medium was performed in YPLactate medium (1% yeast extract, 1% peptone, 2% (w/v) lactic acid pH5.3). For starvation experiments, unless otherwise stated, cultures in selective medium were inoculated in YPD medium and maintained in exponential growth phase for at least five generations; cells were harvested by centrifugation, washed with distilled water and autophagy was induced by inoculation in YNB medium without ammonium sulfate and amino acid ($-NH_3$-aa) for nitrogen starvation, or YNB medium without amino acid ($+NH_3$-aa) for amino acid starvation. For ammonium starvation experiments, ($-NH_3$ + aa), yeast cells were inoculated in YNB without ammonium sulfate but supplemented with histidine (10mg/L), tryptophane (10mg/L), leucine (50mg/L), methionine (10mg/L) and lysine (15mg/L) ($-NH_3$+aa). Autophagy induction with rapamycin was achieved with rapamycin 200nM.

To obtain rho^0 mutants, a culture of RS4Δ grown to saturation on YPD medium containing ethidium bromide (10µg/mL) was diluted and re-inoculated at low density in the same medium. The resulting respiratory deficiency was confirmed by a complete lack of growth on YPLactate medium which is an obligatory respiratory medium.

GFP-Atg8 cleavage assay and other western blot analyses

The GFP-Atg8 cleavage assay takes advantage of the fact that GFP-Atg8, covalently attached to the autophagosome membrane, follows the autophagy flux until cleavage in the vacuole, where GFP resists further proteolysis [21]. Approximately 10^8 cells were harvested, and lysed by alkaline whole cell extraction (0.2M NaOH; 0.3% β-mercaptoethanol) followed by trichloroacetic acid precipitation [7]. Protein extracts were subsequently washed with acetone, dried and suspended in 100µL of 5% (w/v) SDS. Finally, 100µL of Laemmli buffer (20% glycerol, 2% SDS, 2% β-mercaptoethanol, 0.04% Bromophenol Blue, 0.0625M Tris-HCl pH6.8) were added. Samples were incubated for 10min at 65°C prior to loading for electrophoresis on a 12% polyacrylamide gel. Routinely, lysate aliquots corresponding to $4x10^6$ cells were analyzed. After western blotting onto nitrocellulose and blocking the membrane with 5% non-fat milk, 0.1% Tween 20 in Tris-buffered saline, the blotted proteins were probed with mouse anti-GFP antibody (1/2000, Roche Applied Science, Meylan), followed by HRP conjugated anti-mouse IgG secondary antibody (1/10000, Jackson-Interchim). Detection was performed with ECL prime from GE Healthcare. Other western blot analyses were performed on similar extracts, using the appropriate acrylamide gel concentrations (8% or 12%) and the appropriate primary and secondary antibodies. These included mouse monoclonal anti-Pgk1 antibodies (1/10000, Invitrogen), mouse monoclonal anti-HA antibodies (1/2000, Santa Cruz), rabbit anti-phospho eIF2a (1/1500, Thermofisher Scientific), and HRP conjugated anti-rabbit or -mouse IgG secondary antibody (1/10000, Jackson-Interchim).

RNA extraction, reverse transcription (RT) and real-Time PCR

Nucleic acids were extracted from $2x10^8$ cells as already described [22], then RNA was selectively precipitated in 3M LiCl final (25min on ice, then 16,000xg for 30min at 4°C),

washed with 70% cold ethanol, air-dried and resuspended in nuclease-free water. RNA was quantified (OD 260 nm) and adjusted to 0.25µg/µL. For cDNA synthesis, 1µg of total RNA was incubated for 2h at 37°C with Moloney Murine Leukemia Virus Reverse Transcriptase (M-MLV RT; Promega) and 0.1ng oligo-dT_{25}. The RT reaction was terminated on ice by 1/5 dilution in double-distilled water. For each sample, a control reaction was run without reverse transcriptase to estimate the amount of contaminating DNA. Real-time qPCR made use of a LightCycler® apparatus and SYBR Green mix (Roche Applied Science, Meylan, France), with the primers listed in Table 1. Each primer pair gave a single PCR product by melting curve analysis and agarose gel electrophoresis. The PCR steps were: enzyme activation at 95°C for 10min followed by 40 cycles (for *ACT1*) or 45 cycles (for *PCL5*, *HIS4* and *ATG1*) comprising 10s at 95°C, 10s at 60°C (*ACT1*) or 65°C (*HIS4*) or 66°C (*PCL5* and *ATG1*), and 10s (*ACT1*) or 20s (*PCL5*, *HIS4* and *ATG1*) at 72°C. PCR reactions on non reverse-transcribed RNA samples indicated that genomic DNA contaminants were always less than 1/100. *ACT1* was used as the reference gene and the relative changes in target genes mRNA levels were calculated from ΔCt values.

Fluorescence microscopy

Microscopy was performed on a FV1000 Olympus confocal microscope using a 100X oil immersion lens (NA 1.40) coupled to a 2.0X numerical zoom (0.08µm per pixel). The excitation wavelengths for GFP or FM4-64 were set to 488nm and 543nm respectively. Image acquisition and conversion were performed separately for green (520nm) and red (603nm) channels and processed with the Olympus Fluoview version 4.1 software. Transmission images were acquired with differential interference contrast optics.

Vacuoles were visualised by overnight staining with FM4-64 (1µM) in complete medium prior to the shift in starvation medium.

Results and discussion

Amino acid starvation inhibits autophagy in lipid droplet-deficient cells

Previous reports have shown that rapamycin efficiently induced autophagy in RS4Δ cells, whereas nitrogen starvation failed to do so [7, 9]. Here, both stimuli were combined in our experiments and autophagy completion was assessed by the GFP-Atg8 cleavage assay [21]. We observed that rapamycin-induced autophagy was completely inhibited by nitrogen starvation (Fig. 1A compare "Rap" and "-N+Rap"). Because nitrogen starvation is a combination of deficiencies in amino acids and in ammonium ion, both conditions were analyzed separately. In this experimental paradigm, autophagy could be observed when ammonium deficiency was imposed in the presence of amino acids (Fig. 1B), whereas amino acid starvation in the presence of ammonium ion failed to activate autophagy (Fig. 1B). As above, the combination of both deficiencies did not induce autophagy (Fig. 1B). Amino acid starvation also proved sufficient to block rapamycin-induced autophagy (Fig. 1C). The addition of increasing doses of the auxotrophic amino acids progressively restored rapamycin-induced autophagy, with a threshold observed around 1% of the standard amino acid supply (Fig. 1C). Similarly, ammonium starvation-induced autophagy was restored by amino acids in a dose-dependent manner, with a threshold around 10% of the standard amino acid supply (Fig. 1D). Together our data indicate that, in lipid droplet-deficient yeast, amino acid deficiency not only failed to induce autophagy but also blocked the effects of two signals that induce autophagy through direct inhibition of TORC1. In fact, rapamycin inhibits TORC1 after forming a complex with FKBP12 (FK506 binding protein) [23] and ammonium ion deficiency causes a drop in glutamine concentration, an amino acid acutely required for the activity of the TORC1 complex [24]. In contrast, a deficiency in auxotrophic amino acids

inhibits TORC1 more indirectly, through the activation of TORC2, which activates Gcn2, which in turn inhibits TORC1 [25, 26].

Starvation sensing is functional in lipid droplet-deficient cells

TORC1 represses autophagy through phosphorylation of the Atg13 protein [20]. When TORC1 is inhibited, Atg13 adopts a partially dephosphorylated form that initiates autophagy by recruiting Atg1 [27, 28]. We therefore examined whether amino acid starvation altered the efficiency of Atg13 dephosphorylation in lipid droplet-deficient cells. This hypothesis was not supported by our western blot analysis because ammonium starvation, amino acid starvation and rapamycin had similar effects on Atg13 dephosphorylation (Fig. 2A). This result suggested that the autophagy blockade caused by amino acid starvation did not take place at the initiation step. Because TORC1 inhibition by amino acid deficiency requires the activation of Gcn2 [15], the result also suggested that this indirect pathway was functional in RS4Δ cells. Gcn2 is a component of the GAAC pathway that plays a central role in the adaptation of yeast and animal cells to a reduction in amino acid supply [29]. In this pathway, Gcn2 senses amino acid depletion and phosphorylates the translation regulator eIF2alpha (eukaryotic initiation factor), resulting in an accumulation of the transcription factor Gcn4 that in turn activates the expression of several genes required for amino acid synthesis [30]. In addition, Gcn4 increases *ATG1* expression [31] and is specifically required for autophagy in response to amino acid starvation [15]. Therefore, we examined whether the functionality of the GAAC pathway was altered in lipid droplet-deficient cells. Our experiments indicated that eIF2α phosphorylation was stimulated in all conditions of ammonium and/or amino acid starvation (Fig. 2B), thus confirming the functionality of Gcn2 in the GAAC pathway. Furthermore, transcriptional activation of three Gcn4-responsive genes, including *ATG1* [31], could be observed after ammonium and/or amino acid starvation, indicating that the GAAC

pathway was fully operational in lipid droplet-deficient cells (Fig. 2C). Together, our experiments indicated that Gcn2 fulfilled all its autophagy-related tasks in lipid droplet-deficient yeast (*i.e.* Atg13 dephosphorylation and induction of *ATG1*). Nevertheless, considering the prominent role of Gcn2 in amino acid depletion sensing and the diversity of effectors it may control [32], we felt compelled to examine whether the absence of lipid droplet might confer upon it the ability to inhibit autophagy downstream of Atg13 and Atg1. Such a paradoxical situation could be ruled out because *GCN2* deletion did not relieve the inhibitory effect of amino acid starvation on rapamycin-induced autophagy (Fig. 2D). This result further indicates that the mechanism of autophagy inhibition in amino acid-starved RS4Δ cells does not rely on Gcn2 to sense amino acid depletion. Having ruled out this central actor of cell adaptation to amino acid starvation, we explored other routes that could lead to autophagy inhibition.

Autophagy inhibition in lipid droplet-deficient cells is sensitive to the redox state of the cells

The mitochondrial respiratory chain plays a role when autophagy is induced by amino acid starvation [33]. We sought to examine mitochondrial shape following autophagy induction in RS4Δ cells. Using plasmid pSu9-GFP as a reporter of mitochondrial shape, we observed that mitochondrial morphology in RS4Δ cells was differentially affected in response to amino acid deficiency and/or ammonium limitation. As shown in Fig.3A, 90% of the cells in the RS4Δ strain contained compact mitochondrial aggregates, clustered in one or two spots, when the cells were challenged by amino acid starvation for 2 hours. This shape is strikingly similar to the *mdm* (mitochondrial distribution and morphology) mutants, some of which are respiratory deficient [34]. The mitochondrial aggregates are clearly excluded from the vacuole ruling out the possibility that they result from mitophagy (Supplemental Figure 2). In response to ammonium starvation, RS4Δ displayed a less severe phenotype since aggregated

mitochondria were observed in only 43% of the cells. None of these starved conditions altered the typical tubular morphology of mitochondria in wild type cells (Fig. 3A). To substantiate the correlation between mitochondria integrity and autophagic ability in RS4Δ, we generated a RS4Δ rho^0 mutant and analyzed autophagy in response to nitrogen starvation. Rho^0 mutants lack all the components encoded by mitochondrial DNA and are thus unable to produce mitochondrial ATP. Interestingly, mitochondrial DNA ablation exacerbated the phenotype of RS4Δ since RS4Δ rho^0 proved unable to accomplish autophagy even in response to ammonium starvation (Fig. 3B). Importantly, autophagy was still observed in the rho^0 lipid droplet-proficient strain in response to ammonium starvation as reported before [33]. We concluded from these experiments that lipid droplet-deficient cells are more dependent on functional mitochondria than the wild type strain for autophagy in response to starvation.

Previous studies have shown that nitrogen - or amino acid - starvation leads to a transient increase in mitochondrial respiration, even in glucose medium [35]. Moreover, the production of ROS (reactive oxygen species) along the respiratory chain appears to be required for optimal activation of autophagy [36, 37]. Having established that amino acid deficiency altered mitochondrial function in RS4Δ, we questioned whether the autophagic phenotype of RS4Δ resulted from failure to generate ROS. As illustrated in figure 3C, addition of 0.3-0.5mM H_2O_2 facilitated autophagy in response to nitrogen starvation and to a lesser extent, to amino acid starvation. H_2O_2 alone did not significantly activate autophagy (Fig. 3C). H_2O_2 concentrations above 0.5mM had a toxic effect characterized by a reduced autophagy and the presence of multiple protein degradation bands. Additional evidence for a strong influence of the redox state on autophagy in RS4Δ cells could be obtained by showing that autophagy in response to ammonium ion deficiency was obliterated by the addition of the ROS scavenger N-acetylcysteine (Fig. 3D). The same concentrations of N-acetylcysteine did not abolish autophagy in lipid droplet-proficient cells (Fig. 3D). Together, the data are in

keeping with our previous report indicating that RS4Δ displays a high GSH (glutathione reduced form)/GSSG (glutathione oxidised form) ratio [38]. This increased ROS buffering capacity in RS4Δ cells might dampen the burst of ROS production that is required for autophagy [36]. The fact that the addition of H_2O_2 facilitated autophagy but did not fully restore it suggests that ROS production was not the only contribution of mitochondria to the autophagic process. This prompted us to turn to experimental protocols that allow full restoration of mitochondrial function.

Autophagy in lipid droplet-deficient cells is highly dependent on mitochondrial status

We then examined whether autophagy could be restored in RS4Δ cells by culture conditions that favour mitochondria proliferation and activity. For this purpose, cells were grown in lactic acid media. In this fully respiratory medium, lipid droplet-deficient cells showed essentially the same growth-rate as wild type cells, although the growth rate of both strains was reduced by 50% as compared to fermentative conditions. Taking into account this growth delay, autophagy was monitored over 8 hours. Western blot analysis indicated the RS4Δ mutant was able to execute autophagy in response to the different combinations of ammonium and/or amino acid starvation (Fig. 4A, left panel). Comparison with the wild type strain (Fig. 4A, right panel) revealed that the autophagy at 8 hours was nearly as intense in the RS4Δ mutant. A delayed autophagy could be observed in the mutant at 4 hours in the groups lacking amino acids (Fig. 4A, compare left and right panels). To obtain additional evidence, GFP-Atg8-expressing RS4Δ cells were examined by fluorescence microscopy after 6h of ammonium and/or amino acid starvation in respiratory growth conditions. In 70-100% of the cells, the GFP signal was either restricted to the vacuole (vacuolar) or encompassing the vacuole and the cytosol (uniform) (Fig. 4B). We interpreted these results as indicative of a completed autophagy or an autophagic flux in progress, respectively (Fig. 4B). For

311 comparison, effective autophagy in response to rapamycin in glucose medium resulted in 90%
312 of the cells with GFP entirely or partially vacuolar, whereas autophagy blockade in glucose
313 medium lacking both ammonium and amino acids yielded only 10% of that score (Fig. 4B).
314 Taken together, our results indicated that autophagy was restored to near wild type levels in
315 lactate-grown RS4Δ cells. Consistent with these results, the tubular morphology of the
316 mitochondria was not affected by amino acid shortage in respiratory medium (Supplemental
317 Figure 3). Because previous studies have indicated that RS4Δ cells generate ER membrane
318 tangles during autophagy failure [7-9], we examined the effect of respiration on this process.
319 To observe accurately the ER membrane, the ER-resident protein Sec63 was epitope-tagged
320 with GFP (Supplemental Figure 4 and 5). Using Sec63-GFP, fluorescence membrane tangles
321 could be observed in nearly all the cells upon nitrogen starvation in glucose medium (Fig. 4C,
322 left panel), whereas they were extremely rare in respiratory medium (Fig. 4C, right panel).
323 Therefore, respiration was also effective in resolving this other dysfunction of nitrogen-
324 starved RS4Δ cells. In fermentable medium, mitochondria production is limited by the
325 catabolic repression pathway, which is highly dependent on the phosphatase regulatory
326 subunit Reg1 [39]. Deletion of the *REG1* gene in RS4Δ cells efficiently abolished the
327 inhibitory effect of amino acid starvation on autophagy induced by ammonium starvation in
328 glucose-grown cells (Fig. 4D). Moreover, amino acid starvation *per se* proved capable of
329 inducing autophagy in this mutant (Fig. 4D). To further substantiate this conclusion, we
330 analyzed GFP-Atg8 localisation in the RS4Δ-*reg1Δ* by fluorescence microscopy. As
331 illustrated in Figure 4B, upon ammonium or amino acid starvation, GFP fluorescence reached
332 the vacuole in more than 80% of the cells. Thus, *REG1* deletion restored the autophagic
333 turnover of GFP-Atg8 in glucose medium. Because *REG1* deletion causes both an increase in
334 mitochondria biomass and ATP production by respiration even in fermentative medium, we
335 sought to separate the structural and metabolic contributions of mitochondria to autophagy

restoration. As illustrated in Fig. 4E, RS4Δ-*reg1Δ* rho^0 cells remained capable of activating autophagy in all conditions of ammonium and/or amino acid starvation. A slight decrease in GFP-Atg8 cleavage (compare Fig. 4D and E) may represent the loss of ROS contribution to autophagy restoration, although it also lies within the range of western blot variability.

In this report, we clarify the origin of the autophagy failure observed in lipid droplet-deficient cells by showing that it is singularly due to a toxic effect of amino acid starvation. Despite our best efforts, the amino acid starvation sensor that triggers this toxic effect has not been identified, although we were able to exonerate the GAAC pathway. We have been more successful at identifying the role of aggregated mitochondria in the mechanism of autophagy inhibition. This new information complements previous reports indicating that a rise in fatty acid synthesis was responsible for the autophagy blockade in lipid droplet-deficient cells challenged by nitrogen starvation [7, 9]. It could be anticipated that excess fatty acid was not the only cause of autophagy inhibition, because pharmacological correction of fatty acid synthesis merely achieved partial restoration of autophagy [7, 9]. In contrast, we show here that autophagy can be restored to near wild type level by increasing mitochondria activity and biomass (*i.e.* respiration or ablation of the *REG1* gene). Interestingly, although we observed that ROS production along the respiratory chain facilitated autophagy, the RS4Δ-*reg1Δ* rho^0 cells remained capable of activating autophagy upon amino acid starvation. Therefore, it would appear that mitochondria biomass and structural integrity are more meaningful than respiration for the restoration of autophagy. A noticeable correlate of autophagy inhibition in lipid droplet-deficient cells is an accumulation of tangled ER membranes whose mechanism remains to be elucidated [7, 9]. We would like to speculate that these tangled ER membranes may arise as a consequence of the mitochondrial aggregation described herein. They could, in fact, result from an interruption of phosphatidylserine transfer from the ER to the outer

mitochondrial membrane where it normally gets converted to phosphatidylethanolamine in the phospholipid synthesis pathway [40, 41]. This could explain why pharmacological correction of fatty acid synthesis, as performed in previous studies, only achieved partial restoration of autophagy while it completely resolved the ER tangles [7]. In contrast, rescuing mitochondria through respiration efficiently restored both autophagy and ER integrity. Thus, progress made in characterizing the autophagy failure in lipid droplet-deficient cells directs future studies towards a possible role of lipid droplets in the membrane contacts connecting mitochondria and ER. It can be hypothesized that the ER-mitochondria encounter structure (ERMES) [41] requires the presence of lipid droplets to function adequately when fatty acid synthesis is increased by amino acid starvation. In support of this hypothesis, a similar situation seems to arise at the nuclear ER-vacuolar junction (NVJ) where lipid droplets are recruited upon increased fatty acid concentration, so as to ensure neutral lipid storage, which in turn prevents excessive phospholipids synthesis and the formation of ER tangles [42]. Further analysis of the autophagy failure in lipid droplet-deficient yeast may thus provide a more general view of the mechanisms involved in organelle contacts and ER homeostasis.

Acknowledgements

This work has been funded by the French Ministry of Research. It has benefited from the facilities and expertise of the ImageUP platform (University of Poitiers). We are grateful to Anne Cantereau for her support for confocal imaging. We would like to thank Jenny Colas (STIM Poitiers) for her technical assistance. We are also very grateful to Roger Schneiter (University of Fribourg) for providing the yeast strain RS4Δ, to Paul Hermann (Ohio State University), to Hiromi Sesaki (John Hopkins University) and to Nadine Camougrand (CNRS and Université de Bordeaux) for providing plasmids. We are very grateful to Dr Jemma M. Buck and Graham Buck for proofreading and English-editing the manuscript.

Declarations of interest

The authors declare no conflict of interest

Author contribution

MR, PV designed the research: MB, MR and PV performed the experiments; TB, MB, MR and PV analyzed data; MR and PV wrote the paper with comments from TB and MB.

References

1 Yang, Z. and Klionsky, D. J. (2010) Eaten alive: a history of macroautophagy. Nature cell biology. **12**, 814-822

2 Tsukada, M. and Ohsumi, Y. (1993) Isolation and characterization of autophagy-defective mutants of Saccharomyces cerevisiae. FEBS letters. **333**, 169-174

3 Weidberg, H., Shvets, E. and Elazar, Z. (2011) Biogenesis and cargo selectivity of autophagosomes. Annual review of biochemistry. **80**, 125-156

4 Mari, M., Tooze, S. A. and Reggiori, F. (2011) The puzzling origin of the autophagosomal membrane. F1000 biology reports. **3**, 25

5 Dupont, N., Chauhan, S., Arko-Mensah, J., Castillo, E. F., Masedunskas, A., Weigert, R., Robenek, H., Proikas-Cezanne, T. and Deretic, V. (2014) Neutral lipid stores and lipase PNPLA5 contribute to autophagosome biogenesis. Current biology : CB. **24**, 609-620

6 Li, D., Song, J. Z., Li, H., Shan, M. H., Liang, Y., Zhu, J. and Xie, Z. (2015) Storage lipid synthesis is necessary for autophagy induced by nitrogen starvation. FEBS letters. **589**, 269-276

7 Regnacq, M., Voisin, P., Sere, Y. Y., Wan, B., Soeroso, V. M. S., Bernard, M., Camougrand, N., Bernard, F. X., Barrault, C. and Berges, T. (2016) Increased fatty acid synthesis inhibits nitrogen starvation-induced autophagy in lipid droplet-deficient yeast. Biochemical and biophysical research communications. **477**, 33-39

8 Shpilka, T., Welter, E., Borovsky, N., Amar, N., Mari, M., Reggiori, F. and Elazar, Z. (2015) Lipid droplets and their component triglycerides and steryl esters regulate autophagosome biogenesis. The EMBO journal. **34**, 2117-2131

9 Velazquez, A. P., Tatsuta, T., Ghillebert, R., Drescher, I. and Graef, M. (2016) Lipid droplet-mediated ER homeostasis regulates autophagy and cell survival during starvation. The Journal of cell biology. **212**, 621-631

10 Meyers, A., Weiskittel, T. M. and Dalhaimer, P. (2017) Lipid Droplets: Formation to Breakdown. Lipids. **52**, 465-475

11 Sandager, L., Gustavsson, M. H., Stahl, U., Dahlqvist, A., Wiberg, E., Banas, A., Lenman, M., Ronne, H. and Stymne, S. (2002) Storage lipid synthesis is non-essential in yeast. The Journal of biological chemistry. **277**, 6478-6482

12 Garbarino, J., Padamsee, M., Wilcox, L., Oelkers, P. M., D'Ambrosio, D., Ruggles, K. V., Ramsey, N., Jabado, O., Turkish, A. and Sturley, S. L. (2009) Sterol and diacylglycerol acyltransferase deficiency triggers fatty acid-mediated cell death. The Journal of biological chemistry. **284**, 30994-31005

13 Petschnigg, J., Wolinski, H., Kolb, D., Zellnig, G., Kurat, C. F., Natter, K. and Kohlwein, S. D. (2009) Good fat, essential cellular requirements for triacylglycerol synthesis to maintain membrane homeostasis in yeast. The Journal of biological chemistry. **284**, 30981-30993

14 Rockenfeller, P., Ring, J., Muschett, V., Beranek, A., Buettner, S., Carmona-Gutierrez, D., Eisenberg, T., Khoury, C., Rechberger, G., Kohlwein, S. D., Kroemer, G. and Madeo, F. (2010) Fatty acids trigger mitochondrion-dependent necrosis. Cell cycle. **9**, 2836-2842

15 Ecker, N., Mor, A., Journo, D. and Abeliovich, H. (2010) Induction of autophagic flux by amino acid deprivation is distinct from nitrogen starvation-induced macroautophagy. Autophagy. **6**, 879-890

16 Gueldener, U., Heinisch, J., Koehler, G. J., Voss, D. and Hegemann, J. H. (2002) A second set of loxP marker cassettes for Cre-mediated multiple gene knockouts in budding yeast. Nucleic acids research. **30**, e23

17 Janke, C., Magiera, M. M., Rathfelder, N., Taxis, C., Reber, S., Maekawa, H., Moreno-Borchart, A., Doenges, G., Schwob, E., Schiebel, E. and Knop, M. (2004) A versatile toolbox for PCR-based tagging of yeast genes: new fluorescent proteins, more markers and promoter substitution cassettes. Yeast. **21**, 947-962

18 Sesaki, H., Dunn, C. D., Iijima, M., Shepard, K. A., Yaffe, M. P., Machamer, C. E. and Jensen, R. E. (2006) Ups1p, a conserved intermembrane space protein, regulates mitochondrial shape and alternative topogenesis of Mgm1p. The Journal of cell biology. **173**, 651-658

19 Noda, T., Matsuura, A., Wada, Y. and Ohsumi, Y. (1995) Novel system for monitoring autophagy in the yeast Saccharomyces cerevisiae. Biochemical and biophysical research communications. **210**, 126-132

20 Stephan, J. S., Yeh, Y. Y., Ramachandran, V., Deminoff, S. J. and Herman, P. K. (2009) The Tor and PKA signaling pathways independently target the Atg1/Atg13 protein kinase complex to control autophagy. Proceedings of the National Academy of Sciences of the United States of America. **106**, 17049-17054

21 Shintani, T. and Klionsky, D. J. (2004) Cargo proteins facilitate the formation of transport vesicles in the cytoplasm to vacuole targeting pathway. The Journal of biological chemistry. **279**, 29889-29894

22 Li, J., Liu, J., Wang, X., Zhao, L., Chen, Q. and Zhao, W. (2009) A waterbath method for preparation of RNA from Saccharomyces cerevisiae. Analytical biochemistry. **384**, 189-190

23 Cardenas, M. E. and Heitman, J. (1995) FKBP12-rapamycin target TOR2 is a vacuolar protein with an associated phosphatidylinositol-4 kinase activity. The EMBO journal. **14**, 5892-5907

24 Stracka, D., Jozefczuk, S., Rudroff, F., Sauer, U. and Hall, M. N. (2014) Nitrogen source activates TOR (target of rapamycin) complex 1 via glutamine and independently of Gtr/Rag proteins. The Journal of biological chemistry. **289**, 25010-25020

25 Vlahakis, A., Lopez Muniozguren, N. and Powers, T. (2016) Calcium channel regulator Mid1 links TORC2-mediated changes in mitochondrial respiration to autophagy. The Journal of cell biology. **215**, 779-788

26 Yuan, W., Guo, S., Gao, J., Zhong, M., Yan, G., Wu, W., Chao, Y. and Jiang, Y. (2017) General Control Nonderepressible 2 (GCN2) Kinase Inhibits Target of Rapamycin Complex 1 in Response to Amino Acid Starvation in Saccharomyces cerevisiae. The Journal of biological chemistry. **292**, 2660-2669

27 Cheong, H., Yorimitsu, T., Reggiori, F., Legakis, J. E., Wang, C. W. and Klionsky, D. J. (2005) Atg17 regulates the magnitude of the autophagic response. Molecular biology of the cell. **16**, 3438-3453

28 Kabeya, Y., Kamada, Y., Baba, M., Takikawa, H., Sasaki, M. and Ohsumi, Y. (2005) Atg17 functions in cooperation with Atg1 and Atg13 in yeast autophagy. Molecular biology of the cell. **16**, 2544-2553

29 Dong, J., Qiu, H., Garcia-Barrio, M., Anderson, J. and Hinnebusch, A. G. (2000) Uncharged tRNA activates GCN2 by displacing the protein kinase moiety from a bipartite tRNA-binding domain. Molecular cell. **6**, 269-279

30 Hinnebusch, A. G. (2005) Translational regulation of GCN4 and the general amino acid control of yeast. Annual review of microbiology. **59**, 407-450

31 Bernard, A., Jin, M., Xu, Z. and Klionsky, D. J. (2015) A large-scale analysis of autophagy-related gene expression identifies new regulators of autophagy. Autophagy. **11**, 2114-2122

32 Castilho, B. A., Shanmugam, R., Silva, R. C., Ramesh, R., Himme, B. M. and Sattlegger, E. (2014) Keeping the eIF2 alpha kinase Gcn2 in check. Biochimica et biophysica acta. **1843**, 1948-1968

33 Graef, M. and Nunnari, J. (2011) Mitochondria regulate autophagy by conserved signalling pathways. The EMBO journal. **30**, 2101-2114

34 Dimmer, K. S., Fritz, S., Fuchs, F., Messerschmitt, M., Weinbach, N., Neupert, W. and Westermann, B. (2002) Genetic basis of mitochondrial function and morphology in Saccharomyces cerevisiae. Molecular biology of the cell. **13**, 847-853

35 Knupp, J., Martinez-Montanes, F., Van Den Bergh, F., Cottier, S., Schneiter, R., Beard, D. and Chang, A. (2017) Sphingolipid accumulation causes mitochondrial dysregulation and cell death. Cell death and differentiation. **24**, 2044-2053

36 Kissova, I., Deffieu, M., Samokhvalov, V., Velours, G., Bessoule, J. J., Manon, S. and Camougrand, N. (2006) Lipid oxidation and autophagy in yeast. Free radical biology & medicine. **41**, 1655-1661

37 Scherz-Shouval, R., Shvets, E., Fass, E., Shorer, H., Gil, L. and Elazar, Z. (2007) Reactive oxygen species are essential for autophagy and specifically regulate the activity of Atg4. The EMBO journal. **26**, 1749-1760

38 Sere, Y. Y., Regnacq, M., Colas, J. and Berges, T. (2010) A Saccharomyces cerevisiae strain unable to store neutral lipids is tolerant to oxidative stress induced by alpha-synuclein. Free radical biology & medicine. **49**, 1755-1764

39 Schuller, H. J. (2003) Transcriptional control of nonfermentative metabolism in the yeast Saccharomyces cerevisiae. Current genetics. **43**, 139-160

40 Kojima, R., Endo, T. and Tamura, Y. (2016) A phospholipid transfer function of ER-mitochondria encounter structure revealed in vitro. Scientific reports. **6**, 30777

41 Kornmann, B., Currie, E., Collins, S. R., Schuldiner, M., Nunnari, J., Weissman, J. S. and Walter, P. (2009) An ER-mitochondria tethering complex revealed by a synthetic biology screen. Science. **325**, 477-481

42 Hariri, H., Speer, N., Bowerman, J., Rogers, S., Fu, G., Reetz, E., Datta, S., Feathers, J. R., Ugrankar, R., Nicastro, D. and Henne, W. M. (2019) Mdm1 maintains endoplasmic reticulum homeostasis by spatially regulating lipid droplet biogenesis. The Journal of cell biology. **218**, 1319-1334

516 TABLE 1 Oligonucleotides used in this study

517

Name :	Sequence :
GCN2KO forward	TGATTTTTTTTTTCAATAATTTTCCGTTCCCCTTAACACATACTATGTAT AACAGCTGAAGCTTCGTACGC
GCN2KO reverse	TATACTTTACCTTTAACTGATGCGTTATAGCGCCGCACAGATCTTTAAA GGCGCATAGGCCACTAGTGGATCTG
REG1KO forward	ATAAATCCTAAAGCAAGCATATTGACGAAGACGAGATAAGAAAAATC CAAAACAGCTGAAGCTTCGTACGC
REG1KO reverse	ACACTACCTGGATTTTTATTTTCTCTTCATGTTGACTTCAAAATTCTTTC TTGCATAGGCCACTAGTGGATCTG
S2-SEC63	ATATACGTCTAAGAGCTAAAATGAAAAACTATACTAATCACTTATATC TAATCGATGAATTCGAGCTCG
S3-SEC63	ATACTGATATCGATACGGATACAGAAGCTGAAGATGATGAATCACCA GAACGTACGCTGCAGGTCGAC
PCL5 forward	TCCACTGGCAGAAATCCGTATC
PCL5 reverse	GACACCTCTGGATTGGTGAATC
HIS4 forward	AGCTGAAGAACTGACTGAGGC
HIS4 reverse	TGGATTGGTCTGCTCAAAGCC
ATG1 forward	ATTCATTGGCAGACGAGGTTGC
ATG1 reverse	AATCTCGTTGATGCAATACCGAG
ACT1 forward	CCGGTGATGGTGTTACTC
ACT1 reverse	CAAATCTCTACCGGCCAAAT

518

519

520 **Figure legends**

521

522 **Figure 1. Amino acid deficiency inhibits autophagy in lipid droplet-deficient yeast.**

523 **A)** At time T_0 RS4Δ cells expressing GFP-Atg8 were transferred to nitrogen-free medium (-

524 N: without amino acids and without ammonium sulfate) or treated with rapamycin (Rap) in

525 either YPD or nitrogen-free medium. The GFP-Atg8 cleavage test indicated that nitrogen

526 starvation failed to induce autophagy and also blocked the effect of rapamycin. **B)** RS4Δ cells

527 expressing GFP-Atg8 were subjected to ammonium starvation, amino acid starvation, or both.

528 Ammonium starvation induced autophagy in the presence of amino acids, whereas amino acid

529 starvation failed to induce autophagy and also blocked the effect of ammonium starvation. **C)**

530 RS4Δ cells expressing GFP-Atg8 were treated with rapamycin in medium containing

531 ammonium ion and increasing doses of the auxotrophic amino acids (expressed as fractions of

532 the standard supply). **D)** RS4Δ cells expressing GFP-Atg8 were subjected to ammonium

533 starvation in the presence of increasing doses of the auxotrophic amino acids (expressed as

534 fractions of the standard supply).

535 PGK: phosphoglycerate kinase 1 immunodetection as loading standard.

536

537 **Figure 2. Amino acid deficiency sensing in lipid droplet-deficient yeast.**

538 **A)** RS4Δ cells expressing Atg13-HA under the *CUP1* promoter were subjected to ammonium

539 and/or amino acid starvation for 1h, or treated with rapamycin in YPD medium. The

540 phosphorylated and dephosphorylated forms of Atg13-HA were separated on an 8%

541 acrylamide gel and detected with anti-HA antibody. Compared to untreated cells (T_0), all

542 treatments caused Atg13-HA dephosphorylation, indicating the initiation of autophagy is

543 functional in RS4Δ cells. The vertical line delineates different exposures of the same blot. **B)**

544 RS4Δ cells were subjected to ammonium and/or amino acid starvation and examined on

western blot for eIF2α phosphorylation. All treatments yielded the same level of eIF2α phosphorylation. PGK: phosphoglycerate kinase 1 immunodetection as loading standard. The vertical line delineates different exposures of the same blot. **C)** RS4Δ cells were subjected to the indicated treatments and the mRNA levels of three Gcn4 effector genes were quantified by real time RT-qPCR, using actin mRNA as normalizing standard. Error Bars indicate Mean +/- sd. **D)** A paradoxical inhibition of autophagy by the general amino acid control pathway could be ruled out, as amino acid deficiency completely inhibited autophagy to rapamycin in RS4Δ *gcn2*Δ cells. GFP-Atg8 cleavage assay. PGK: phosphoglycerate kinase 1 immunodetection as loading standard.

Figure 3. Mitochondrial status in lipid droplet-deficient cells.

A) RS4Δ or Y10000 cells expressing mitochondria-targeted Su9-GFP [18] were grown to exponential phase on complete medium (YPD) and shifted to either nitrogen-free (-NH_3-aa), or ammonium-free (-NH_3) or amino acid-free (-aa) media for 2h and mitochondria morphology was analyzed by confocal microscopy. Left panel contains representative images of tubular and aggregated mitochondria. Quantification of mitochondria aggregation is presented in the right panel, based on > 200 cells for each experimental group. Scale bar: 5μm.

B) RS4Δ rho^0 cells expressing GFP-Atg8 were starved as indicated and processed through the GFP-Atg8 cleavage assay. The absence of a functional respiratory chain inhibits autophagy to ammonium starvation in RS4Δ cells. **C)** RS4Δ cells expressing GFP-Atg8 were starved for either nitrogen (-NH_3-aa), or amino acid (-aa), or cultured in complete medium YPD for 4h in the presence of the indicated concentration of H_2O_2. Western blot analysis of GFP-Atg8 cleavage indicates that H_2O_2 (0.3-0.5mM) partially restores autophagy in starvation media but does not induce it in complete medium. The vertical line delineates boundary in a composite

image generated from two different blots. **D)** N-acetylcysteine (NAC) treatment blocks GFP-Atg8 processing by autophagy in RS4Δ and but not in Y10000.

PGK: phosphoglycerate kinase 1 immunodetection as loading standard.

Figure 4. Respiration or release from catabolite repression restores autophagy in lipid droplet-deficient cells.

A) RS4Δ (left panel) or Y10000 (right panel) expressing GFP-Atg8 were cultured in YP-Lactate medium. At time T_0, cells were subjected to the indicated starvations in YNB lactic acid media and autophagy was monitored over 8h by GFP-Atg8 cleavage assay. Respiratory conditions restored autophagy to near wild type level in RS4Δ.

B) RS4Δ, Y10000 or RS4Δ-*reg1Δ* expressing GFP-Atg8 were cultured in complete glucose medium or lactate medium as indicated, in the presence of FM4-64 (1μM), and shifted in the same medium lacking either nitrogen (-N) or ammonium ($-NH_3$) or amino acid (-aa), or containing 200nM rapamycin (R) for 6 hours. Cells were examined by confocal microscopy. Left panel contains representative images of the cytosolic, vacuolar or uniform GFP fluorescence in the cells. Quantification of GFP localization in each experimental group is presented in the right panel, based on > 200 cells for each group. Scale bar: 2μm. **C)** RS4Δ cells containing an integrated copy of the ER resident membrane protein Sec63 tagged with GFP were grown in complete medium containing glucose or lactate as the sole carbon source as indicated. Cells were shifted in the same medium lacking nitrogen and the GFP signal was observed. Arrows: tangled membranes. Scale bar: 5μm. **D)** RS4Δ-*reg1Δ* cells expressing GFP-Atg8 were cultured in complete glucose medium, shifted atT_0 to the indicated starvation media and analyzed by GFP-Atg8 cleavage assay. **E)** RS4Δ-*reg1Δ* rho^0 cells expressing GFP-Atg8 were treated as described in D.

PGK: phosphoglycerate kinase 1 immunodetection as loading standard.

595

Figure 1

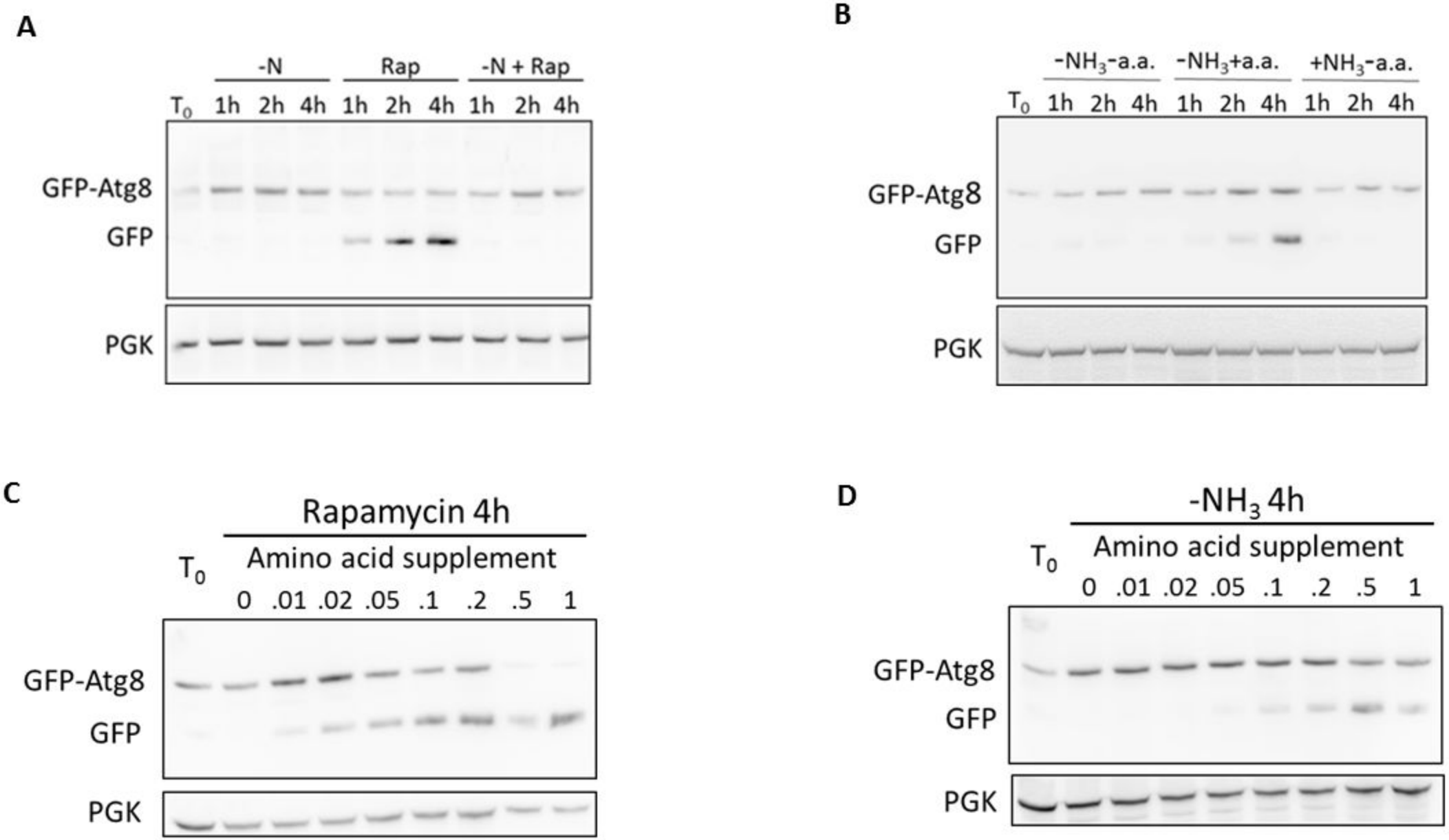
A
-N
Rap
-N + Rap
T0 1h 2h 4h 1h 2h 4h 1h 2h 4h
GFP-Atg8
GFP
PGK
B
-NH3-a.a.
-NH3+a.a.
+NH3-a.a.
T0 1h 2h 4h 1h 2h 4h 1h 2h 4h
GFP-Atg8
GFP
PGK
C
Rapamycin 4h
Amino acid supplement
T0 0 .01 .02 .05 .1 .2 .5 1
GFP-Atg8
GFP
PGK
D
-NH3 4h
Amino acid supplement
T0 0 .01 .02 .05 .1 .2 .5 1
GFP-Atg8
GFP
PGK

A

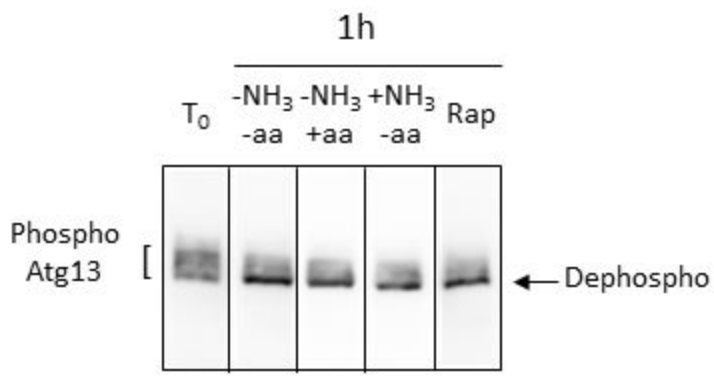
1h
T0
-NH3 -aa
-NH3 +aa
+NH3 -aa
Rap
Phospho Atg13
Dephospho

B

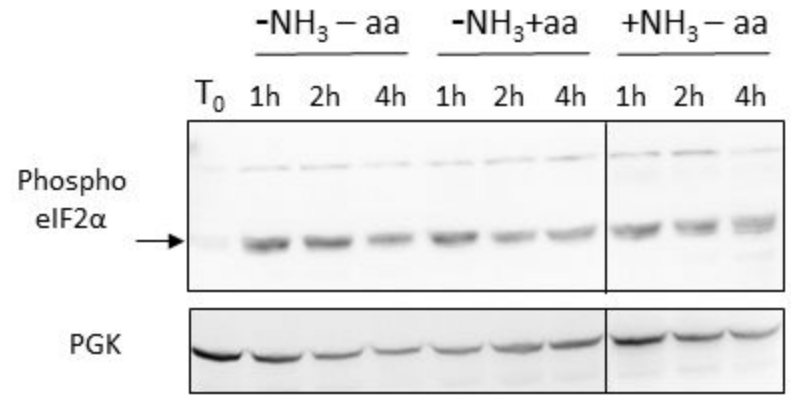
-NH3 – aa
-NH3+aa
+NH3 – aa
T0 1h 2h 4h 1h 2h 4h 1h 2h 4h
Phospho eIF2α
PGK

C

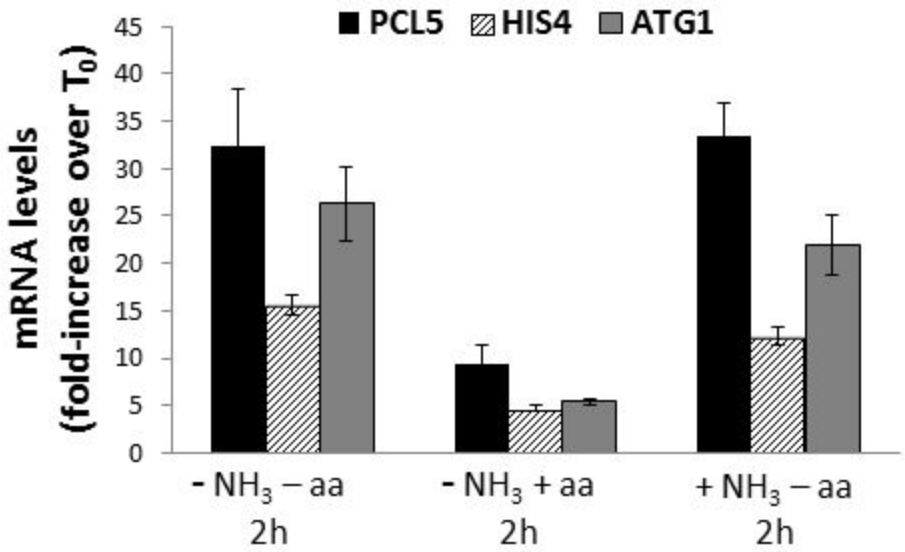
PCL5
HIS4
ATG1
mRNA levels (fold-increase over T0)
45
40
35
30
25
20
15
10
5
0
- NH3 – aa 2h
- NH3 + aa 2h
+ NH3 – aa 2h

D

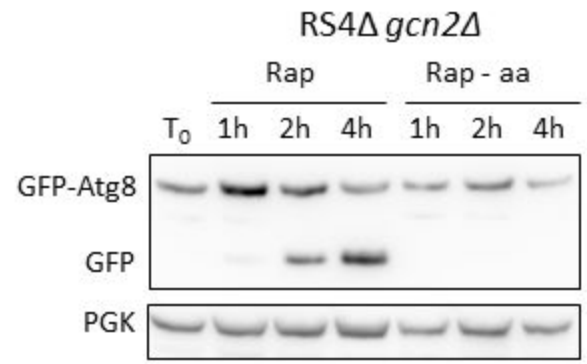
RS4Δ gcn2Δ
Rap
Rap - aa
T0 1h 2h 4h 1h 2h 4h
GFP-Atg8
GFP
PGK

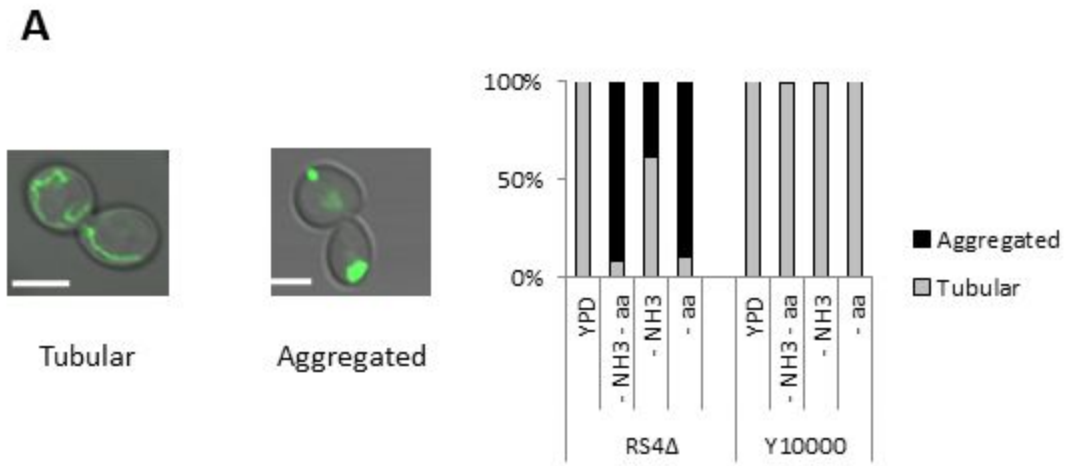
A
Tubular
Aggregated
100%
50%
0%
YPD
- NH3 - aa
- NH3
- aa
YPD
- NH3 - aa
- NH3
- aa
RS4Δ
Y10000
Aggregated
Tubular

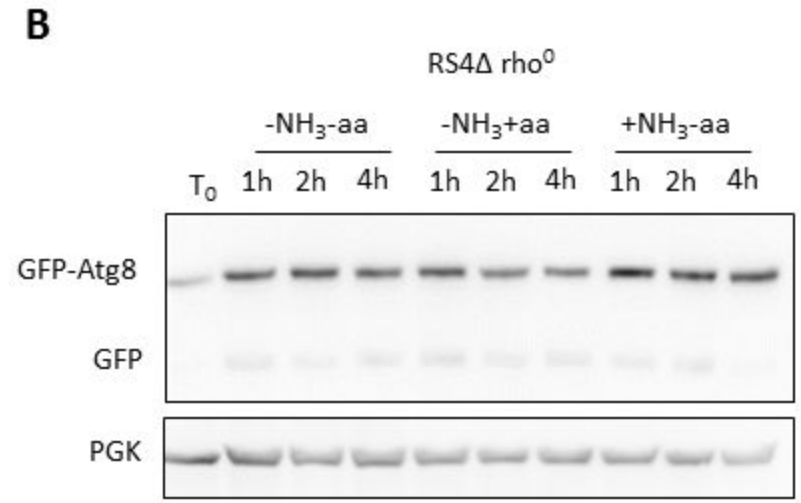
B
RS4Δ rho0
-NH3-aa
-NH3+aa
+NH3-aa
T0 1h 2h 4h 1h 2h 4h 1h 2h 4h
GFP-Atg8
GFP
PGK

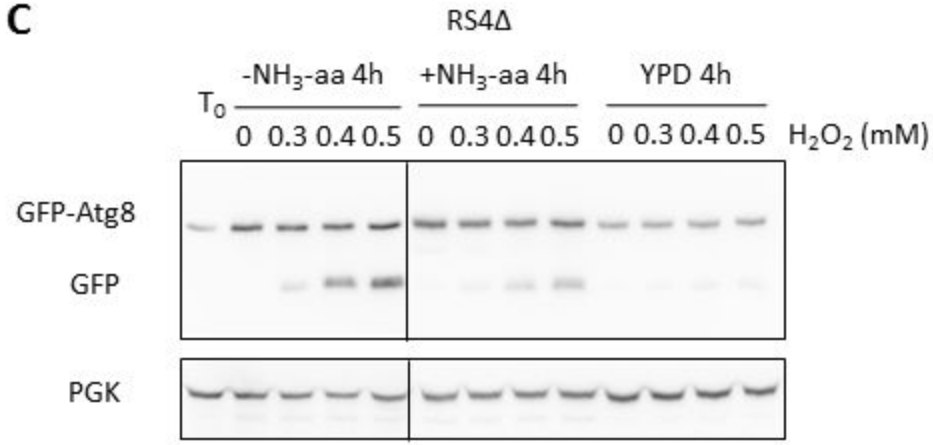
C
RS4Δ
-NH3-aa 4h
+NH3-aa 4h
YPD 4h
T0
0 0.3 0.4 0.5 0 0.3 0.4 0.5 0 0.3 0.4 0.5
H2O2 (mM)
GFP-Atg8
GFP
PGK

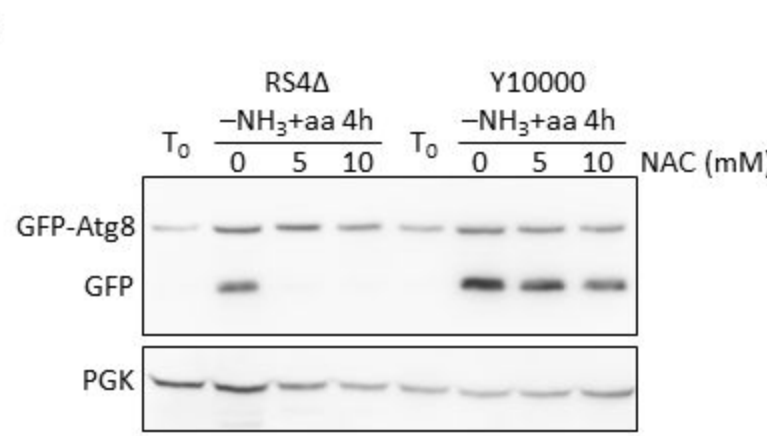
D
RS4Δ
Y10000
–NH3+aa 4h
–NH3+aa 4h
T0 0 5 10 T0 0 5 10
NAC (mM)
GFP-Atg8
GFP
PGK

Figure 4

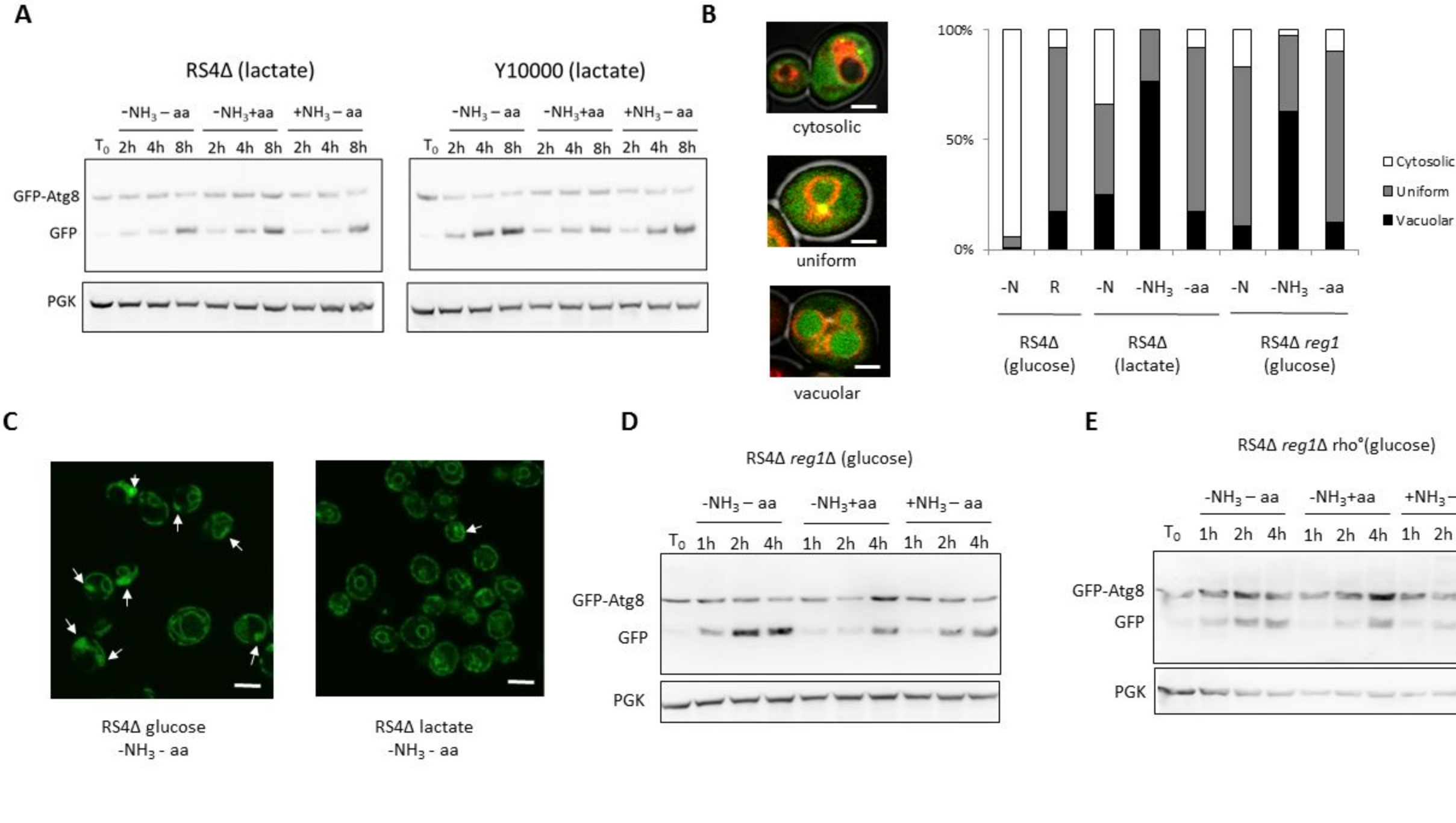
A
RS4Δ (lactate)
Y10000 (lactate)
-NH3 – aa
-NH3+aa
+NH3 – aa
T0 2h 4h 8h 2h 4h 8h 2h 4h 8h
GFP-Atg8
GFP
PGK
B
cytosolic
uniform
vacuolar
100%
50%
0%
Cytosolic
Uniform
Vacuolar
-N R -N -NH3 -aa -N -NH3 -aa
RS4Δ (glucose)
RS4Δ (lactate)
RS4Δ reg1 (glucose)
C
RS4Δ glucose -NH3 - aa
RS4Δ lactate -NH3 - aa
D
RS4Δ reg1Δ (glucose)
T0 1h 2h 4h 1h 2h 4h 1h 2h 4h
GFP-Atg8
GFP
PGK
E
RS4Δ reg1Δ rho°(glucose)
T0 1h 2h 4h 1h 2h 4h 1h 2h 4h
GFP-Atg8
GFP
PGK

Supplemental Figure legends

Supplemental Figure 1. RS4Δ strain does not contain lipid droplets.

Y10000 (left panel) and RS4Δ (right panel) cells were incubated for 10 minutes with 1.5µg/mL Bodipy 493/503 and analyzed by confocal microscopy. Scale bar: 5µm.

Supplemental Figure 2. Mitochondria aggregates are formed in response to nitrogen starvation in RS4Δ.

Y10000 (top panels) and RS4Δ (bottom panels) cells expressing Su9-GFP and stained with FM4-64 were grown in complete medium (left panels) or subjected to nitrogen starvation for 2h (right panels) and analyzed by confocal microscopy. Scale bar: 5µm.

Supplemental Figure 3. Mitochondrial status is normal in lipid droplet-deficient cells after amino acid starvation in respiratory medium.

RS4Δ cells expressing Su9-GFP and stained with FM4-64 were grown in YP lactic medium (top panels) or subjected to amino acid starvation for 2h (bottom panels) and analyzed by confocal microscopy. Left panels: transmission image; middle panel: confocal image of a middle plane of the cells; right panel: confocal image of the top of the cells. Scale bar: 5µm.

Supplemental Figure 4. Sec63-GFP patches correlate with ER membrane tangles in RS4Δ.

A) RS4Δ cells expressing Sec63-GFP were grown to exponential phase in YPD medium and analyzed by confocal microscopy. Scale bar: 5µm. **B)** Same experiment performed with cells subjected to nitrogen starvation for 2h. White arrows indicate several patches of Sec63-GFP fluorescence. Scale bar: 5µm. **C**) Same experiment as in **B** in the presence of cerulenin that

prevents accumulation of ER membrane tangles [7]. Only one patch of Sec63-GFP is observed (white arrow). Scale bar: 5µm. **D and E)** RS4Δ cells were treated as in B and C respectively and processed for electron microscopy: as observed before with confocal microscopy, ER tangles were detected only in the absence of cerulenin. We interpreted these experiments as indicating that Sec63-GFP patches represent ER membrane tangles.

Figure 5. Sec63-GFP patches are connected to the ER.

Optically sliced images from top (1) to bottom (8) of RS4Δ cells expressing Sec63-GFP and subjected to nitrogen starvation. Arrows point to connections between ER and Sec63-GFP patches. Bottom right: transmission image of the corresponding cells. Scale bar: 5µm.